EUROPEAN FUSION DEVELOPMENT AGREEMENT

EFDA–JET–CP(04)03-44

M.E. Puiatti, M. Valisa, L. Garzotti, P. Mantica, A. Bortolon, L. Carraro,
I. Coffey, D. Kalupin, M. Mattioli, M. Tokar, H. Weisen
and JET EFDA Contributors

Relationship between Core Impurity, Fuel and Thermal Diffusivities in L and H-mode JET Plasmas

Relationship between Core Impurity, Fuel and Thermal Diffusivities in L and H-mode JET Plasmas

M.E. Puiatti[1], M. Valisa[1], L. Garzotti[1], P. Mantica[4], A. Bortolon[1], L. Carraro, I. Coffey[2], D. Kalupin[3], M. Mattioli[1], M. Tokar[3], H. Weisen and JET EFDA Contributors*

[1]Consorzio RFX - Associazione Euratom-Enea sulla Fusione, I-35127 Padova, Italy
[2]EURATOM/UKAEA Fusion Association, Culham Science Centre, Abingdon, Oxon, OX14 3DB, UK
[3]IPP, Forschungszentrum Jülich GmbH, EURATOM Association, D-52425 Jülich, Germany
[4]IFP- Istituto di Fisica del Plasma- CNR-EURATOM , 20125Milano, Italy
[5]CRPP, Ecole Polytechnique Fédérale de Lausanne CH-1015 Switzerland
** See annex of J. Pamela et al, "Overview of Recent JET Results and Future Perspectives", Fusion Energy 2002 (Proc. 19th IAEAFusion Energy Conference, Lyon (2002).*

Preprint of Paper to be submitted for publication in Proceedings of the 31st EPS Conference,
(London, UK. 28th June - 2nd July 2004)

INTRODUCTION

Impurity densities are a key factor in the determination of a reactor performance. If the viability of a radiation shield generated at the edge by seeding impurities to dissipate convective losses is a matter of debate, the presence of impurities in the core is clearly undesired because of the deleterious consequences of radiation losses and plasma dilution on fusion reactivity. In particular the accumulation of impurities and the associated risk of disruptions cannot be tolerated.

A figure of merit in this context is the ratio of the transport parameters of the impurities to those of main fuel and energy. In the published literature D_{imp}/χ_e, or more often τ_{imp}/τ_{Ee}, is reported to vary widely, depending on a variety of parameters such as elongation, triangularity, q_{95}, [1] and is theoretically predicted to be ~ 1 in case of electrostatic turbulent transport [2]. In this paper we analyse the ratios D_{imp}/χ_e and, to a lesser extent, D_{imp}/D_D in a group of JET discharges devised to probe heat and particle (main gas and impurities) diffusivities by means of transient perturbations; namely, electron heating modulation, shallow pellet injection and laser ablation of nickel targets, respectively.

1. THE EXPERIMENT

Several L-mode and ELMy H-mode JET discharges have been analysed: their main characteristics are summarised in the table below. Electron heating modulation was obtained by applying mode converted ICH and adding ~20% of He^3[3].

Pulse No:	B_T (T)	I_P (MA)	n_e (10^{19} m^{-3})	T_e (keV)	T_i (keV)	NBI (MW)	ICRH (MW)	ρ_{ICRH}
55802	3.45	1.85	3.0	6.3	3.1	3.2	3.6	0.13
55804	3.36	1.6	2.8	3.7	2.8	0	3.5	0.18
55805	3.36	1.6	2.8	4.4	3.5	3.2	3.6	0.18
55807	3.25	1.6	2.8	3.5	3.5	6.0	3.7	0.32
55809	3.25	1.6	2.7	4.0	4.0	9.1	3.7	0.32
58149	**3.28**	**1.8**	**3.4**	**5.2**	**5.0**	**14.3**	**2.8**	**0.37**
58143	**3.28**	**1.8**	**3.0**	**5.7**	**4.5**	**13.4**	**2.8**	**0.37**

2. ANALYSIS TOOLS

2.2 HEAT TRANSPORT ANALYSIS

The heat pulse propagation analysis of the L-mode shots was detailed in [3]. It qualified the degree of stiffness of Te according to a critical gradient empirical model. More specifically Pulse No: 55802, featuring electron heating in the core ($\rho_{ICRH} = 0.13$) resulted above the critical gradient for $\rho > 0.1$, while Pulse No's: 55809 and 58149, with a more external electron heat deposition ($\rho_{ICRH} = 0.32$ and 0.37) were above stiffness for $\rho > 0.3$ and $\rho > 0.35$ respectively.

2.2 IMPURITY TRANSPORT ANALYSIS

Transport parameters of Ni following laser ablation have been deduced by means of a 1D-impurity transport model [4] that simulates available Ni spectroscopic lines, inverted soft-X-ray brightness and bolometer data. As boundary condition the time behaviour of a NI XIII emission line is tracked. The intrinsic carbon behaviour has also been considered, essentially for the calculation of the

neoclassical transport of Ni by means of NCLASS [5]. To avoid subjective criteria a minimisation procedure has been used to converge to the best choice of transport parameters and identify a degree of confidence of the results. Unlike other cases, in the shots here analysed it has not been necessary to modify transport parameters during the penetration phase and the subsequent decay phaseof the Ni pulse; one single couple of diffusivity and convection has been adequate for a satisfactory simulation of the whole sequence.

3. DEUTERIUM TRANSPORT ANALYSIS

Transport parameters of deuterium have been analysed for shots 55802, 55809 by means of the JETTO transport code [6].

3.1STABILITY ANALYSIS

To correlate the experimentally deduced transport parameters with the underlying instabilities the collisionless linear stability code KINEZERO has been used [7] in the regions where the applicability criteria are met.

4. RESULTS

4.1 L MODE.

Diffusivity D_{Ni} and convection *v* of nickel of two L-mode shots are plotted in Fig.1 together with χ_e from the heat modulation analysis as well as D_D and v_D from the he analysis of pellet. Neoclassical diffusion, including the effect of the presence of carbon, is much smaller than the experimental one. D_{Ni} in Pulse No: 55802 is everywhere higher than in Pulse No: 55809. Also, in Pulse No: 55802 the low diffusion region in the core is narrower than in Pulse No: 55809. In both discharges the pinch velocity is inward all along the radius and of several m/s, much higher than the neoclassical one. In analogy with D_{Ni} a central low convection region seems to be present in both shots, narrower in Pulse No: 55802. χ_e and D_{Ni} show several similarities; in particular they share the radius at which a transition in transport occurs.

The difference of transport in the two L mode discharges can be also qualitatively grasped from the contour plots of the inverted SXR emissivity (Fig. 2) that clearly shows how Ni penetrates much faster in shot 55802 and how the penetration speed in both cases slows down at about the radius where D_{Ni} drops and where also the electron temperature critical gradient is crossed [3]. Simulations of the effects of the shallow deuterium pellet have shown that the diffusion of the deuterium is comparable to that of Ni; the pinch velocity of D is lower than that of Ni but the shape is similar.

4.2 H-MODE

In the H-mode example (Fig.3) χ_e and D_{Ni} are also similar with a transition from low to high transport around r/a=0.35 (for this shot χ_e is taken from a similar Pulse No:, Pulse No: 58148, without Ni LBO). The pinch velocity is about 1 m/s, lower than in the L-mode shots. The effective outward pinch in the core is required to simulate a SXR radial profile less peaked than the temperature

one. The neoclassical contribution to diffusivity is negligible. Neoclassical convection remains lower than the effective one. D_D is still to be analysed.

DISCUSSION

The close relationship between χ_e and D_{Ni} shown above can perhaps be emphasised recalling the main results of the heat diffusivity analysis of the same shots [3]. Indeed D_{Ni} is high or low depending on where the electron temperature gradient is above or below the critical threshold, just like heat diffusivity. To stress the analogy, we observe that, as found for the stiffness level [8], in the region above the critical threshold D_{Ni} appears to depend on the ion temperature inverse gradient length R/L_{Ti} (Fig.4). The differences in shots 55802 and 55809 mirror the different spatial distribution of the dominating electrostatic instabilities. Figure 5 shows the maximum growth rates γ of ITG/TEM instabilities as a function of minor radius. For both L-mode shots and for toroidal wavenumber $n <$ 100 (corresponding to ITG/TEM instabilities) γ is sizeable just at the radius where the transport transition occurs. We mention that in Pulse No: 55802 also some ETG activity ($n > 100$) shows up in the centre (not shown in Fig.5).

CONCLUSIONS

Ni LBO injections in shots where also transient perturbations of density and electron temperature were available have shown that: D_{Ni} and v_{Ni} are highly anomalous in the analysed L-mode and H-mode discharges; $D_{Ni} \sim \chi_e$; nickel and deuterium have similar diffusion in the plasma core; D_{Ni} profiles are well correlated with the profiles of electron temperature inverse gradient length, showing transition from low to high transport when the critical value found for electron heat is exceeded. This behaviour is also consistent with that of the maximum growth rates of electrostatic ITG/TEM instabilities.

ACKNOWLEDGEMENTS

C. Bourdelle's help in dealing with Kinezero is kindly acknowledged.

REFERENCES

[1]. M.Mattioli et al Nucl. Fus. 35 (1995) 1115 **&** M.R. Wade et al. Phys. Plasmas, 2 (1995) 2357 **&** E. Scavino et al. Plasma Phys and Contr. Fus., **45** (2003), 1961

[2]. X. Garbet, "*Physics of anomalous transport in Tokamaks* ", this conference

[3]. P.Mantica et al. IAEA 2002, EX/P1-04 **&** P.Mantica et al., EPS 2003, vol.27A-O3.1A

[4]. M.Mattioli et al., J. Phys. B **34** (2001) 127

[5]. W.A. Houlberg et. Al. , Phys. of Plasmas, 4 (1997) 3230

[6]. Cenacchi G Taroni A, Report ENEA-RT-T113-88-5

[7]. C. Bourdelle et al., Nucl. Fus. **42** (2002) 892

[8]. P. Mantica et al, " *Predictive Modelling of Te modulation experiments in JET Lmode and H mode plasmas"* this conference.

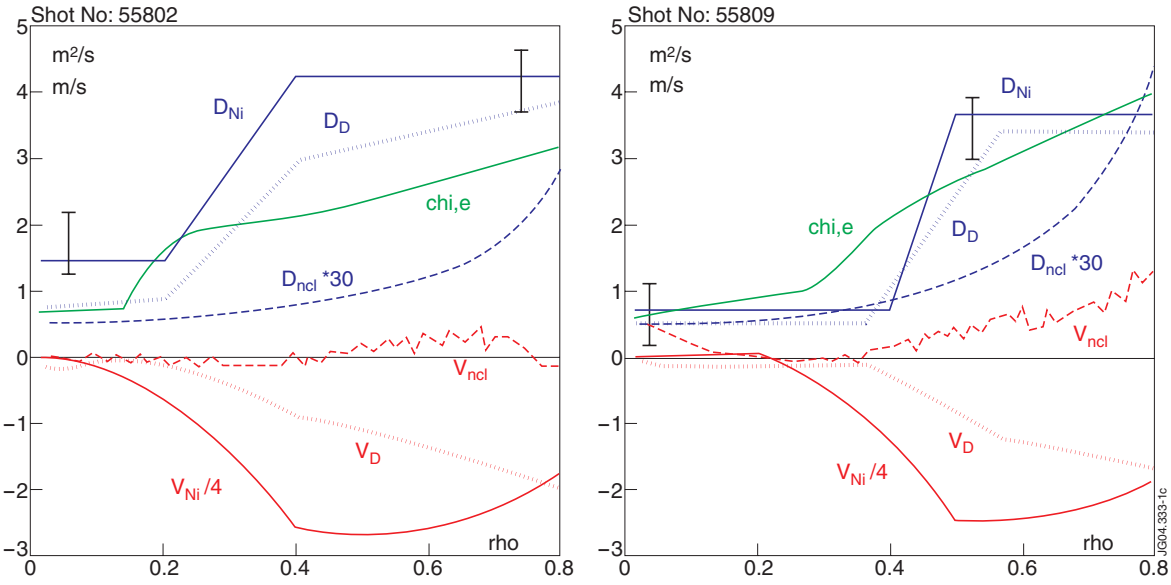

Figure 1: Effective and neoclassical nickel D_{Ni} and v_{Ni}, χ_e in green from heat modulation analysis, D_D and V_D from pellet analysis for the two L-mode shots. Error bars on the diffusion of Ni are only a degree of confidence of the simulation.

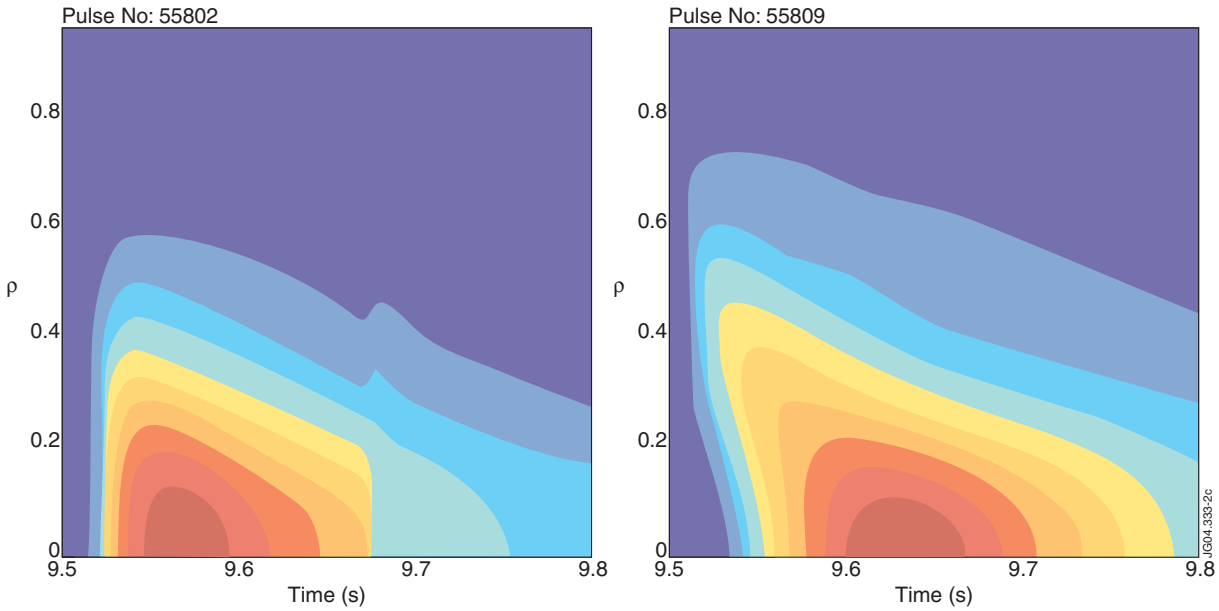

Figure 2: Contour plots of the inverted SXR emissivity versus time: Ni penetrates at 9.5sec much faster in Pulse No: 55802.

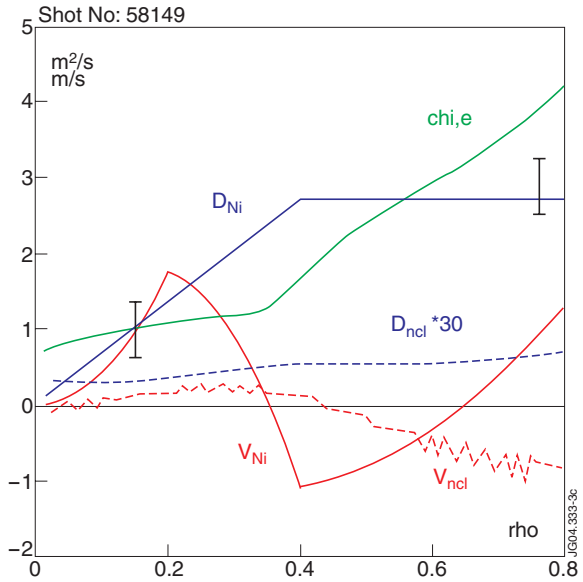

Figure 3: Effective and neoclassical nickel diffusion and convection and χ_e for the H mode shot.

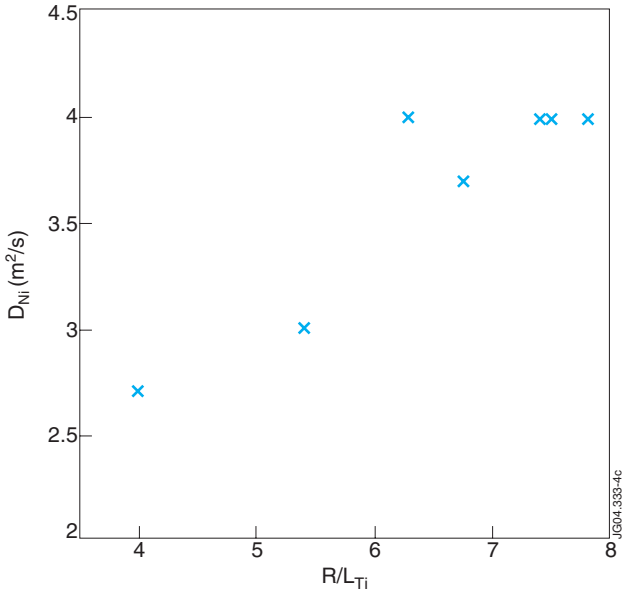

Figure 4: Dependence of D_{Ni} in the stiff region on R/L_{Ti} for the seven analysed shots.

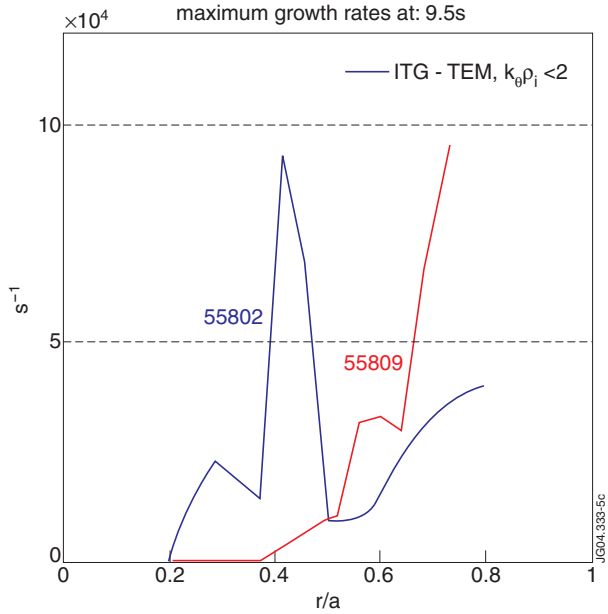

Figure 5:Growth rates of the dominating instabilities, for $k_\theta r_{I,}$ <2 from KINEZERO as a function of the minor radius, in the range 0.2< r/a<0.8.